Mode Matching Method for Photonic Crystal Slabs

Aasmund S. Sudbø
University of Oslo, University Graduate Center - UNIK
N-2027 KJELLER, Norway, email: aas@unik.no +47 6484 4700

November 22, 2010

Abstract

The mode matching method is applied to the calculation of Bloch wave fields in photonic crystal slab structures. The transmitted, reflected and diffracted waved are calculated for an incident plane wave.

1 Introduction

The motivation for the work reported below is the fact that we have coworkers who have fabricated and characterized semiconductor membranes with a 2D-periodic pattern of air holes [1, 2], mebranes that often can be modeled quite accurately by a two-dimensional photonic crystal (2D PC) slab [3]. . We would like to simulate the transmission and reflection of harmonic optical plane waves by such PC slabs or films. Above the PC film, there are incident, reflected, and diffracted waves, each with two possible polarizations. Inside the PC film, we express the optical field as a series expansion of Bloch-wave solutions for the infinitely extruded 2D PC [3]. In the procedure called mode matching, the amplitudes of the terms in the series expansion are adjusted so that the electric and magnetic fields on the top and bottom of the PC film match the fields of the freely propagating fields above and below. The method discussed here is an extension of the mode matching method used in [4, 5, 6, 7] for computing the mode fields of optical waveguides. A structure analyzed with this implemetation of the mode matching method is modeled by a sandwich of M "slices" numbered $m = 1, 2...M$. Each slice is considered to be cut from a two-dimensional photonic crystal (2D PC) that is uniform and infinitely thick in the direction perpendicular to the photonic crystal plane. Hence it is natural to attach the label m not only to slice number m, but also to the infinitely extruded 2D PC that slice no. m is cut from. Also worth noting is the fact that a homogeneous material may be considered to be a photonic crystal, having any desired crystal period. A PC slab or film is a structure where all the slices making up the film have the same 2D PC lattice structure and orientation.

2 Theory

Let us have the photonic crystal film in the x-y-plane. We call the x- and y-directions transverse and the z-direction longitudinal. Then the slices are perpendicular to the z-axis, lying in the x-y-plane, as shown in Fig.1, and both the lattice vectors of the PC and its reciprocal lattice vectors lie in the x-y-plane. We let both z and m increase from the bottom up. Let c be the speed of light, ω the angular frequency, λ the corresponding vacuum wavelength, and k the corresponding angular repetency, so that

$$k_0 = \omega/c = 2\pi/\lambda. \tag{1}$$

Let $\hat{x}$, $\hat{y}$ and $\hat{z}$ denote unit vectors in the x-, y- and z-directions, respectively, let t denote time, and let the position be denoted

$$\mathbf{r} = \vec{r} + z\hat{z} = x\hat{x} + y\hat{y} + z\hat{z}, \tag{2}$$

In the above equation, and in the following, an arrow above a symbol, like in $\vec{r} = x\hat{x} + y\hat{y}$, is used to denote a transverse vector, *i.e.*, a vector in the x-y plane. A 2D photonic crystal is characterized by a relative permittivity

$$\varepsilon^{(m)}\left(\vec{r}\right) = n^{(m)}\left(\vec{r}\right)^2, \tag{3}$$

where $n^{(m)}\left(\vec{r}\right)$ is the refractive index. $\varepsilon^{(m)}\left(\vec{r}\right)$ and $n^{(m)}\left(\vec{r}\right)$ are both independent of z and periodic in the x-y plane:

$$\varepsilon^{(m)}\left(\vec{r}\right) = \varepsilon^{(m)}\left(\vec{r} + \Lambda_x\hat{x}\right) = \varepsilon^{(m)}\left(\vec{r} + \Lambda_y\hat{y}\right), \tag{4}$$

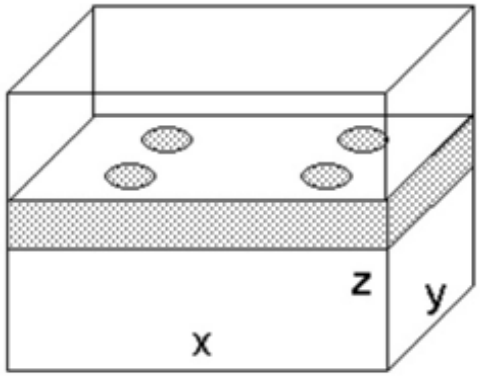

Figure 1: *Simple 3-slice structure consisting of air, a photonic crystal (PC) slice, resting on a homogeneous substrate. Four air holes are indicated in the PC, so two periods of the PC are shown in each direction.*

for any position $\vec{r}$ in the x-y plane. In the general case, the structure of a 2D photonic crystal may be such that $\hat{x}$ and $\hat{y}$ are not perpendicular, but let us limit our discussion to the case where they are perpendicular. Then, we speak about the reciprocal plane, the plane where the transverse Block vectors (BVs) reside:

$$\vec{k} = k_x \hat{x} + k_y \hat{y}. \tag{5}$$

In the reciprocal plane, we have the reciprocal lattice, characterized by the reciprocal lattice vectors,

$$\vec{G}_{l,q} = (2\pi l/\Lambda_x)\,\hat{x} + (2\pi q/\Lambda_y)\,\hat{y}, \tag{6}$$

where l and q are integers. The region at the center of the reciprocal lattice, characterized by

$$-\pi/\Lambda_x < k_x < \pi/\Lambda_x \quad \text{and} \quad -\pi/\Lambda_y < k_y < \pi/\Lambda_y \tag{7}$$

is of particular significance, and is called the first Brillouin zone. We know that we are always free to limit $\vec{k}$ to be in the first Brillouin zone, and that for a given frequency, we may add any reciprocal lattice vector (6) to $\vec{k}$ without any change in the corresponding Bloch wave.

Let the top and bottom slices, no. 1 and no. M, be homogeneous and isotropic, so that we have simple plane-wave solutions for the fields in those two slices. Let us consider the case where we have an incoming propagating harmonic plane wave from the bottom, a wave with wave vector

$$\mathbf{k}_{in}^{(1)} = \vec{k}_{in} + k_{z,in}\hat{z} = k_{x,in}\hat{x} + k_{y,in}\hat{y} + k_{z,in}\hat{z}. \tag{8}$$

The wavelength in slice number 1 is equal to 2π divided by the length of the wave vector $\mathbf{k}_{in}^{(1)}$:

$$\lambda^{(1)} = 2\pi c/\left(n^{(1)}\omega\right) = 2\pi/\left|\mathbf{k}_{in}^{(1)}\right|. \tag{9}$$

where $n^{(1)}$ is the index of refraction of the homogeneous and isotropic material in the bottom slice. Let θ_{in} be the angle between the z axis and the incoming wave vector $\mathbf{k}_{in}^{(1)}$, and let us call this angle the angle of incidence. Then

$$\cos\theta_{in} = k_{z,in}/\left|\mathbf{k}_{in}^{(1)}\right| = k_{z,in}\lambda^{(1)}/(2\pi), \tag{10}$$

In the bottom slice, the x and y components of the E-field (the transverse components) may be written

$$\vec{E}^{(1)}(\vec{r},z,t) = \mathrm{Re}\left[\vec{E}_{l,q;p}^{(1)}\left(\vec{k},\omega\right)\exp\left(i\vec{k}\cdot\vec{r} + ik_{l,q}^{(1)}\left(\vec{k},\omega\right)z - i\omega t\right)\right], \tag{11}$$

and correspondingly for the H-field. The subscript p represents the two possible polarizations for the incoming wave, *i.e.*, $p = H$ for the polarization with nonzero H_z (transverse electric or TE waves), or $p = E$ for the polarization with nonzero E_z (TM waves). The subscripts l and q are integers identifying the various plane-wave solutions that satisfy the Bloch-wave (BW) boundary conditions that are common to all slices of the PC film structure:

$$\vec{E}^{(1)}(\vec{r} - \Lambda_x\hat{x}, z, t)\exp(ik_x\Lambda_x) = \vec{E}^{(1)}(\vec{r}, z, t) = \vec{E}^{(1)}(\vec{r} - \Lambda_y\hat{y}, z, t)\exp(ik_y\Lambda_y). \tag{12a}$$

Regardless of what the 2D PC lattice structure of the PC film is, we can extend the lattice into an adjoining homogeneous slice, and for a plane wave in the homogeneous slice to satisfy (12a), $k_{l,q}^{(1)}$ must satisfy

$$k_{l,q}^{(1)}\left(\vec{k},\omega\right)^2=\left(n^{(1)}\omega/c\right)^2-\left(\vec{k}+\vec{G}_{l,q}\right)^2, \tag{13}$$

where $\vec{G}_{l,q}$ must be a reciprocal-lattice vector (6). We do not need the subscript p on $k_{l,q}^{(1)}$ for a homogeneous and isotropic slice, since $k_{l,q}^{(1)}$ is the same for both polarizations.

Within each slice of the PC film structure we have BW solutions for the fields, where the transverse components of the E-field in slice no. m may be written

$$\vec{E}^{(m)}\left(\vec{r},z,t\right)=\mathrm{Re}\left[\vec{E}_{l,q;p}^{(m)}\left(\vec{k},\omega,\vec{r}\right)\exp\left(i\vec{k}\cdot\vec{r}+ik_{l,q;p}^{(m)}\left(\vec{k},\omega\right)z-i\omega t\right)\right], \tag{14}$$

and correspondingly for the H-field. For a 2D PC in general, the triplet $(l,q;p)$ may be considered just a label distinguishing the various BWs, and a natural ordering of BWs is based on the real part of $k_{l,q;p}^{(m)}\left(\vec{k},\omega\right)^2$, as discussed in detail in [8]. For any BW, the fields $\vec{E}_{l,q;p}^{(m)}\left(\vec{k},\omega,\vec{r}\right)$ and $\vec{H}_{l,q;p}^{(m)}\left(\vec{k},\omega,\vec{r}\right)$ are periodic functions of the position $\vec{r}$ in the x-y-plane, and the Bloch wave has a wave vector called the Bloch vector (BV),

$$\mathbf{k}_{l,q;p}^{(m)}\left(\vec{k},\omega\right)=\vec{k}+k_{l,q;p}^{(m)}\left(\vec{k},\omega\right)\hat{z}. \tag{15}$$

2.1 Metamaterial

In a PC membrane made of a transparent material, $\varepsilon^{(m)}$ is positive and real, and for low frequencies, there are always two BWs with different polarizations, waves with real $k_z=k_{0,0;p}^{(m)}$, representing propagation in the z direction. Each of these two BWs behaves like a plane wave in a homogeneous material, with a wavelength equal to 2π divided by the length of the corresponding Bloch vector $\mathbf{k}_{0,0;p}^{(m)}$:

$$\lambda_{0,0;p}^{(m)}\left(\vec{k},\omega\right)=2\pi/\left|\mathbf{k}_{0,0;p}^{(m)}\right|=2\pi/\sqrt{k_x^2+k_y^2+k_{0,0;p}^{(m)}\left(\vec{k},\omega\right)^2}. \tag{16}$$

Even if the material that the PC membrane is made of is isotropic, an air hole pattern results in anisotropy, so that $\lambda_{0,0;E}^{(m)}$ is in general not equal to $\lambda_{0,0;H}^{(m)}$. To allow us to speak of low frequency, the dimensions of the unit cell of the PC must be much smaller than the wavelength of the two lowest-order BWs:

$$\max\left(\Lambda_x,\Lambda_y\right)\ll\lambda_{0,0;p}^{(m)}/2. \tag{17}$$

The low-frequency limit is also called a metamaterial. In a metamaterial, we do not need to consider any of the possible higher-order Bloch waves in any of the 2D PC slices making up the PC film, and waves propagate in each slice as if it were made of an anisotropic homogeneous material.

2.2 Diffraction

When the field inside the PC film is generated by an incoming plane wave, the transverse Bloch vector $\vec{k}$ is given by the wave vector of the incoming plane wave, as explained above. For a given frequency and $\vec{k}$, the z-component $k_z=k_{l,q;p}^{(m)}\left(\vec{k},\omega\right)$ of a specific BV must be calculated for each BW in slice no. m by solving Maxwells equations in 2D PC no. m.

If both of the periods Λ_x and Λ_y are smaller than or equal to half a wavelength,

$$\max\left(\Lambda_x,\Lambda_y\right)\leqslant\lambda^{(1)}/2, \tag{18}$$

we have a purely reflecting (also called nondiffracting) film, where there is only one reflected and one transmitted wave for each incoming wave. The reflected wave propagates downwards and has wave vector

$$\mathbf{k}_{refl}^{(1)}=\vec{k}_{in}-k_{z,in}\hat{z}=k_{x,in}\hat{x}+k_{y,in}\hat{y}-k_{z,in}\hat{z}. \tag{19}$$

For a nondiffracting film, $\vec{k}_{in}$ is always in the first Brillouin zone. If the film is diffracting, there may be several diffracted waves propagating away from the film, in addition to the directly reflected and transmitted waves. Furthermore, it is possible for the incoming waves to have a propagation directions such that $\vec{k}_{in}$ is not in the first Brillouin zone. If that is the case, we can always find a reciprocal lattice vector $\vec{G}_{in}$ such that

$$\vec{k}=\vec{k}_{in}-\vec{G}_{in} \tag{20}$$

is in the first Brillouin zone.

2.3 Evanescent Bloch Waves

We know that if we have a plane interface between a low-index and a high-index material, we can have propagating fields on the high-index side and evanescent fields (exponentially decaying) on the low-index side of the interface. Eq. (13) shows that in the transparent and homogenous bottom slice, there is a limited number of BWs that are propagating (with real $k_{l,q}^{(1)}\left(\vec{k},\omega\right)$), whereas all high-order BWs are evanescent (with purely imaginary $k_{l,q}^{(1)}\left(\vec{k},\omega\right)$). This classification can be extended to extruded 2D PCs, where there is a limited number of BWs that are propagating (with real $k_{l,q}^{(m)}\left(\vec{k},\omega\right)$), whereas all high-order BWs are evanescent. Furthermore, in an extruded 2D PC we find in general that if we specify $\vec{k}$ and ω, and look at the resulting $k_{l,q;p}^{(m)}$'s, we find an unlimited number of $k_{l,q;p}^{(m)}$'s that are actually complex and not only imaginary, as discussed in detail in [8]. A salient feature of a PC is the existence of band gaps, frequency ranges where only evanescent BWs exist, and the existence of complex evanescent BWs in an extruded 2D PC is intimately related to the existence of band gaps in the PC.

2.4 Bloch Wave Fields

The periodic fields of the Bloch wave (PFBWs) $\vec{E}_{l,q;p}^{(m)}+\hat{z}E_{z;l,q;p}^{(m)}$ and $\vec{H}_{l,q;p}^{(m)}+\hat{z}H_{z;l,q;p}^{(m)}$ are periodic functions of position $\vec{r}$, satisfying the following form of Maxwell's equations:

$$\left(\vec{\nabla}+i\vec{k}\right)\times\vec{E}_{l,q;p}^{(m)} = i\omega\mu_0\hat{z}H_{z;l,q;p}^{(m)}, \tag{21}$$

$$i\omega\varepsilon^{(m)}\vec{E}_{l,q;p}^{(m)} = \hat{z}\times\left[\left(\vec{\nabla}+i\vec{k}\right)H_{z;l,q;p}^{(m)}-ik_{l,q;p}^{(m)}\vec{H}_{l,q;p}^{(m)}\right], \tag{22}$$

$$\left(\vec{\nabla}+i\vec{k}\right)\times\vec{H}_{l,q;p}^{(m)} = -i\omega\varepsilon^{(m)}\varepsilon_0\hat{z}E_{z;l,q;p}^{(m)}, \tag{23}$$

$$\text{and}\quad i\omega\mu_0\vec{H}_{l,q;p}^{(m)} = -\hat{z}\times\left[\left(\vec{\nabla}+i\vec{k}\right)E_{z;l,q;p}^{(m)}-ik_{l,q;p}^{(m)}\vec{E}_{l,q;p}^{(m)}\right]. \tag{24}$$

From these equations it can be shown that

1. If we have an upward propagating Bloch wave (BW) with z-component $k_z=k_{l,q;p}^{(m)}\left(\vec{k},\omega\right)$ of the Bloch vector (BV), we also have a downward propagating BW with $k_z=-k_{l,q;p}^{(m)}\left(\vec{k},\omega\right)$, with the same transverse BV $\vec{k}$ and the same transverse E-field and H-field, except that we have to invert the sign of the transverse H-field. To show this, just replace $k_{l,q;p}^{(m)}$ by $-k_{l,q;p}^{(m)}$ everywhere in the equations, and observe that the original equations may be recovered by changing the sign of three of the six field components.

2. Let us consider a photonic crystal (PC) with inversion symmetry, where $\varepsilon^{(m)}\left(\vec{r}\right)=\varepsilon^{(m)}\left(-\vec{r}\right)$, and where $\varepsilon^{(m)}$ is symmetric about any point along the z axis because it is independent of z. Then the set of equations above is invariant under inversion, in the sense that we get the same set of equations if we invert $\mathbf{r}$, $\mathbf{k}_{l,q;p}^{(m)}$, and $\mathbf{E}_{l,q;p}^{(m)}=\vec{E}_{l,q;p}^{(m)}+\hat{z}E_{z;l,q;p}^{(m)}$. Hence, in a PC with inversion symmetry we have BW pairs, so that if we have a BW with $+\mathbf{k}^{(m)}$, $+\mathbf{E}^{(m)}\left(\mathbf{r},t\right)$, and $+\mathbf{H}^{(m)}\left(\mathbf{r},t\right)$ then we also have a BW with $-\mathbf{k}^{(m)}$, $-\mathbf{E}^{(m)}\left(-\mathbf{r},t\right)$, and $+\mathbf{H}^{(m)}\left(-\mathbf{r},t\right)$.

3. It then follows that in a PC with inversion symmetry, for each k_z there is a pair of BWs where the transverse BVs of the two members of the pair differ only by a sign, and where the transverse E and H fields of one member of the pair are obtained from the fields of the other member by spatial inversion in the x-y-plane (equivalent to a rotation an angle of π in the plane):

$$\vec{E}_{l,q;p}^{(m)}\left(\vec{k},\omega,\vec{r}\right)=\vec{E}_{l',q';p}^{(m)}\left(-\vec{k},\omega,-\vec{r}\right)\quad\text{and}\quad\vec{H}_{l,q;p}^{(m)}\left(\vec{k},\omega,\vec{r}\right)=\vec{H}_{l',q';p}^{(m)}\left(-\vec{k},\omega,-\vec{r}\right). \tag{25}$$

4. A PC is typically fabricated from transparent materials, so that the permittivity ε is real, and then a PFBW corresponding to an inversion of the transverse BV (from $\vec{k}$ to $-\vec{k}$) may be obtained by complex conjugation of the fields:

$$\vec{E}_{l,q;p}^{(m)}\left(-\vec{k},\omega,\vec{r}\right)=\vec{E}_{l,q;p}^{(m)}\left(\vec{k},\omega,\vec{r}\right)^*\quad\text{and}\quad\vec{H}_{l,q;p}^{(m)}\left(-\vec{k},\omega,\vec{r}\right)=\vec{H}_{l,q;p}^{(m)}\left(\vec{k},\omega,\vec{r}\right)^*. \tag{26}$$

5. Eqs. (21)-(24) as given above are not invariant under complex conjugation for evanescent Bloch waves, even if ε is real. Complex conjugation of the equations yields a BW with an inverted transverse BV and

the inverted and complex-conjugated z-component $k_z = -k_{l,q;p}^{(m)*}$. If k_z is purely imaginary, $k_z = -k_z^*$, complex conjugation is equivalent to changing the sign of k_z, and then we do not really get a new BW via complex conjugation. On the other hand, if we have a BW that satisfies (21)-(24) with a truly complex k_z in an arbitrary PC, we have in general no guarantee that there is a BW with $k_z = k_{l,q;p}^{(m)*}$ that satisfies (21)-(24). Reasoning similar to the one under point 4 above, however, does permit us to conclude that if the PC is lossless with inversion symmetry, then there is indeed a BW with $k_z = k_{l,q;p}^{(m)*}$. For a given transverse component $\vec{k}$ of the Bloch vector, there are then four different BWs with the same absolute value of k_z, corresponding to $k_z = \pm k_{l,q;p}^{(m)}$ and $k_z = \pm k_{l,q;p}^{(m)*}$.

2.5 Bloch Wave Series Expansions

The transverse E-field in slice no. m may be written as a sum of Bloch wave components:

$$\vec{E}^{(m)}(\vec{r},z,t) = \mathrm{Re}\sum_{l,q,p} u_{l,q;p}^{(m)}(z)\ \vec{E}_{l,q;p}^{(m)}\left(\vec{k},\omega,\vec{r}\right)\exp\left(i\vec{k}\cdot\vec{r}-i\omega t\right), \tag{27}$$

accompanied by the transverse H-field

$$\vec{H}^{(m)}(\vec{r},z,t) = -\,\mathrm{Re}\sum_{l,q,p} i\left(u_{l,q;p}^{(m)}(z)/k_{l,q;p}^{(m)}\right)\ \vec{H}_{l,q;p}^{(m)}\left(\vec{k},\omega,\vec{r}\right)\exp\left(i\vec{k}\cdot\vec{r}-i\omega t\right). \tag{28}$$

These series expansions contain both upward- and downward-propagating BWs, and upward-increasing and downward-increasing evanescent BWs. Let $z^{(m)}$ be the position of the interface between slices no. m and $m+1$, so that the thickness of slice no. m is

$$d_z^{(m)} = z^{(m)} - z^{(m-1)}, \tag{29}$$

The BW component amplitudes $u_{l,q;p}^{(m)}(z)$ then have the form

$$\begin{aligned} u_{l,q;p}^{(m)}(z) &= u_{l,q;p}^{(m,l,+)}\exp[ik_{l,q;p}^{(m)}(z-z^{(m-1)})] + u_{l,q;p}^{(m,l,-)}\exp[-ik_{l,q;p}^{(m)}(z-z^{(m-1)})] = & (30)\\ &= u_{l,q;p}^{(m,l,E)}\cos[k_{l,q;p}^{(m)}(z-z^{(m-1)})] + iu_{l,q;p}^{(m,l,H)}\sin[k_{l,q;p}^{(m)}(z-z^{(m-1)})], & (31)\end{aligned}$$

with the z-derivatives

$$\begin{aligned} \dot{u}_{l,q;p}^{(m)}(z) &= ik_{l,q;p}^{(m)}u_{l,q;p}^{(m,l,+)}\exp[ik_{l,q;p}^{(m)}(z-z^{(m-1)})] - ik_{l,q;p}^{(m)}u_{l,q;p}^{(m,l,-)}\exp[-ik_{l,q;p}^{(m)}(z-z^{(m-1)})] = & (32)\\ &= ik_{l,q;p}^{(m)}u_{l,q;p}^{(m,l,H)}\cos[k_{l,q;p}^{(m)}(z-z^{(m-1)})] - k_{l,q;p}^{(m)}u_{l,q;p}^{(m,l,E)}\sin[k_{l,q;p}^{(m)}(z-z^{(m-1)})]. & (33)\end{aligned}$$

In (30) and (31) $u_{l,q;p}^{(m,l,+)}$ and $u_{l,q;p}^{(m,l,-)}$ are the complex amplitudes of the BW components propagating upward and downward in slice no. m, at $z = z^{(m-1)}$, whereas $u_{l,q;p}^{(m,l,E)}$ represents the amplitude of the superposition of the two waves, and $ik_{l,q;p}^{(m)}u_{l,q;p}^{(m,l,H)}$ the accompanying z derivatives:

$$\begin{aligned} u_{l,q;p}^{(m,l,E)} &= u_{l,q;p}^{(m,l,+)} + u_{l,q;p}^{(m,l,-)} & (34)\\ \text{and}\quad u_{l,q;p}^{(m,l,H)} &= u_{l,q;p}^{(m,l,+)} - u_{l,q;p}^{(m,l,-)}. & (35)\end{aligned}$$

Note that in these definitions, for a non-propagating (evanescent) BW, $u_{l,q;p}^{(m,l,+)}$ is the amplitude of the upward-decreasing BW (with positive imaginary part of $k_{l,q;p}^{(m)}$), and $u_{l,q;p}^{(m,l,-)}$ is the amplitude of the accompanying downward-decreasing BW. (The reason for this grouping of propagating and evanescent BWs will be presented below.)

Also note that the series expansions (27) and (28) consist entirely of evanescent BWs, except for a few low-order propagating BWs. The high-order BWs are needed to match fields at each slice interface position $z^{(m)}$, but their ampltudes are appreaciable only near the interfaces and not in between, since their contribution decreases exponentially with distance from the interface. Since an extruded 2D PC in general has an unlimited number of BWs with complex $k_{l,q;p}^{(m)}\left(\vec{k},\omega\right)$, the field inside slice no m of the PC film structure may contain superposition of up to 4 different BWs having the same absolute value of k_z, namely $k_z = \pm k_{l,q;p}^{(m)}\left(\vec{k},\omega\right)$ and $k_z = \pm k_{l,q;p}^{(m)}\left(\vec{k},\omega\right)^*$.

Finally, using (30) and (31) we define corresponding amplitudes $u_{l,q;p}^{(m,u,\pm)}$, $u_{l,q;p}^{(m,u,E)}$ and $u_{l,q;p}^{(m,u,H)}$ on the upper side of slice no. m, at $z = z^{(m)}$. It will be convenient to have one symbol to represent either of the two slice side labels l and u; let us use the symbol s for this purpose.

2.6 Impedance and Reflection Coefficients Matrices

Let us introduce vectors $\mathbf{u}^{(m,s,\pm)}$, $\mathbf{u}^{(m,s,E)}$ and $\mathbf{u}^{(m,s,H)}$, with elements $u^{(m,s,\pm)}_{l,q;p}$, $u^{(m,s,E)}_{l,q;p}$, and $u^{(m,s,H)}_{l,q;p}$, respectively. (Note that the $\mathbf{u}$-vectors are mathematical objects, not vectors in 3D physical space). Furthermore, we introduce diagonal matrices $\mathbf{K}^{(m)}$ with diagonal elements

$$K^{(m)}_{(l,q;p),(l,q;p)} = k^{(m)}_{l,q;p} d^{(m)}_z, \tag{36}$$

impedance matrices $\mathbf{Z}^{(m,s)}$ relating $\mathbf{u}^{(m,s;E)}$ and $\mathbf{u}^{(m,s;H)}$,

$$\mathbf{u}^{(m,s;E)} = \mathbf{Z}^{(m,s)} \mathbf{u}^{(m,s;H)}, \tag{37}$$

and reflection coefficient matrices $\mathbf{\Gamma}^{(m,s)}$ relating $\mathbf{u}^{(m,s,-)}$ and $\mathbf{u}^{(m,s,+)}$,

$$\mathbf{u}^{(m,s,-)} = \mathbf{\Gamma}^{(m,s)} \mathbf{u}^{(m,s,+)}, \tag{38}$$

It is straightforward to show from (34), (35), (37), and (38) that

$$\mathbf{Z}^{(m,s)} = \left(\mathbf{I} + \mathbf{\Gamma}^{(m,s)}\right) \left(\mathbf{I} - \mathbf{\Gamma}^{(m,s)}\right)^{-1} \tag{39}$$

$$\text{and} \quad \mathbf{\Gamma}^{(m,s)} = \left(\mathbf{Z}^{(m,s)} - \mathbf{I}\right) \left(\mathbf{Z}^{(m,s)} + \mathbf{I}\right)^{-1}, \tag{40}$$

where $\mathbf{I}$ is the identity matrix. From (30) we obtain

$$\mathbf{u}^{(m,u,\pm)} = \exp\left(\pm i \mathbf{K}^{(m)}\right) \mathbf{u}^{(m,l,\pm)}. \tag{41}$$

Then (41) and (38) yield

$$\mathbf{\Gamma}^{(m,u)} = \exp\left(-i \mathbf{K}^{(m)}\right) \mathbf{\Gamma}^{(m,l)} \exp\left(-i \mathbf{K}^{(m)}\right), \tag{42}$$

which may be combined with (39) and (40) to yield

$$\begin{aligned} \mathbf{Z}^{(m,u)} &= \left[\cos\left(\mathbf{K}^{(m)}\right) \mathbf{Z}^{(m,l)} + i \sin\left(\mathbf{K}^{(m)}\right)\right] \left[i \sin\left(\mathbf{K}^{(m)}\right) \mathbf{Z}^{(m,l)} + \cos\left(\mathbf{K}^{(m)}\right)\right]^{-1} = \\ &= \left[\mathbf{Z}^{(m,l)} + i \tan\left(\mathbf{K}^{(m)}\right)\right] \left[i \tan\left(\mathbf{K}^{(m)}\right) \mathbf{Z}^{(m,l)} + \mathbf{I} \cos\left(\mathbf{K}^{(m)}\right)\right]^{-1} \end{aligned} \tag{43}$$

This formula also holds if the impedances $\mathbf{Z}^{(m,s)}$ are replaced by the admittances $\left(\mathbf{Z}^{(m,s)}\right)^{-1}$.

Let us assume that we have a discrete set of sampling points $\vec{r}$ that yields discrete representations $\vec{E}^{(m)}_{l,q;p}(\vec{r})$ and $\vec{H}^{(m)}_{l,q;p}(\vec{r})$ of the transverse E-and H-fields of each PFBW in slice no. m. These representations may be considered to be matrices $\mathbf{O}^{(m;E)}$ and $\mathbf{O}^{(m;H)}$ with matrix elements $O^{(m;E)}_{(\vec{r},c),(\vec{G},p)}$ and $O^{(m;H)}_{(\vec{r},c),(\vec{G},p)}$, respectively, with $\vec{r}$ running over the spatial positions and c representing either one of the two transverse field components. Ideally, the number of sampling points for the fields should be same as the same as the number of BWs included in the sums (27) and (28), so that $\mathbf{O}^{(m;E)}$ and $\mathbf{O}^{(m;H)}$ are square matrices, and the sampling points should be chosen so that these matrices are nonsingular. Point matching of the transverse E- and H-fields across the interface between slice m and slice $m+1$ then yields

$$\mathbf{O}^{(m+1;E)} \mathbf{u}^{(m+1,l,E)} = \mathbf{O}^{(m;E)} \mathbf{u}^{(m,u,E)} \tag{44}$$

$$\text{and} \quad \mathbf{O}^{(m+1;H)} \mathbf{u}^{(m+1,l,H)} = \mathbf{O}^{(m;H)} \mathbf{u}^{(m,u,H)}. \tag{45}$$

If all the $\mathbf{O}^{(m;E)}$ and $\mathbf{O}^{(m;H)}$ are nonsingular square matrices, we then obtain

$$\mathbf{u}^{(m+1,l,E)} = \left[\mathbf{O}^{(m+1;E)}\right]^{-1} \mathbf{O}^{(m;E)} \mathbf{u}^{(m,u,E)} = \mathbf{O}^{(m+1,m;E)} \mathbf{u}^{(m,u,E)} \tag{46}$$

$$\text{and} \quad \mathbf{u}^{(m+1,l,H)} = \left[\mathbf{O}^{(m+1;H)}\right]^{-1} \mathbf{O}^{(m;H)} \mathbf{u}^{(m,u,H)} = \mathbf{O}^{(m+1,m;H)} \mathbf{u}^{(m,u,H)}, \tag{47}$$

where we have introduced the slice interface coupling matrices $\mathbf{O}^{(m+1,m;E)}$ and $\mathbf{O}^{(m+1,m;H)}$.

Just like in [7, 5], recursion relations may then be deduced for the impedances:

$$\begin{aligned} \mathbf{Z}^{(m+1,l)} &= \mathbf{O}^{(m+1,m;E)} \mathbf{Z}^{(m,u)} \mathbf{O}^{(m,m+1;H)} = \\ &= \mathbf{O}^{(m+1,m;E)} \left[\cos\left(\mathbf{K}^{(m)}\right) \mathbf{Z}^{(m,l)} + i \sin\left(\mathbf{K}^{(m)}\right)\right] \left[i \sin\left(\mathbf{K}^{(m)}\right) \mathbf{Z}^{(m,l)} + \cos\left(\mathbf{K}^{(m)}\right)\right]^{-1} \mathbf{O}^{(m,m+1;H)} \end{aligned} \tag{48}$$

This equation is easily inverted to yield $\mathbf{Z}^{(m,l)}$ expressed by $\mathbf{Z}^{(m+1,l)}$.

Let waves be incident from the bottom. Then we have no waves coming down through the top slice, and no fields that decay exponentially as we go down from the top. We have only the transmitted upward waves and the evanescent fields from the bottom of the top slice, and get the simple boundary condition

$$\mathbf{\Gamma}^{(M,l)} = 0 \quad \text{and } \mathbf{Z}^{(M,l)} = \mathbf{I}. \tag{49}$$

Recursive application of (48) then allows us to compute the impedance matrix $\mathbf{Z}^{(1,l)}$ at the bottom of the bottom slice. The reflection coefficient matrix $\mathbf{\Gamma}^{(1,l)} = \left(\mathbf{Z}^{(1,l)} - \mathbf{I}\right)\left(\mathbf{Z}^{(1,l)} + \mathbf{I}\right)^{-1}$, given by (40) for $m = 1$, then yields the reflected, diffracted, and evanescent plane waves resulting from an incoming plane wave. Finally, we can see the rationale for grouping propagating and evanescent BWs the way we did for the definitions of $u^{(m,l,+)}_{l,q;p}$ and $u^{(m,l,-)}_{l,q;p}$. We need this grouping to get the simple boundary condition (49).

3 Discussion

The formalism above may be used to analyze a number of planar multilayer optical filters incorporating photonic crystal slices as layers of the structure. There is a requirement on the structure in that all layers that are photonic crystal slices have to have the same crystal lattice structure, i.e., the same lattice constants and the same orientation of the lattice axes. Reflection and transmission coefficients for plane waves may be calculated, as a function of optical frequency, angle of incidence with respect to the surface normal, and polarization. In the so-called metamaterial limit, when the wavelength is much larger than either of the two lattice periods of the photonic crystal, there is only one incoming and one reflected wave, but for larger lattice periods, diffraction will be observed, meaning that one incoming plane wave results in outgoing plane waves in addition to the reflected and transmitted plane wave. In general, there may be polarization conversion in reflection, transmission and diffraction, so that the state of polarization of the outgoing waves may be different from that of the incident waves. Such a polarization conversion is also possible in the low-frequency limit, induced by the anisotropy generally observed in a metamaterial.

Any guided resonances of the photonic crystal structure may be found by investigation of the reflection coefficient matrix $\mathbf{\Gamma}^{(1,l)}$ of the bottom slice. The resonances may be found by analyzing the frequency dependence of the elements of this matrix that correspond to propagating (non-evanescent) incoming and reflected waves.

The number of BW components needed in the field expansion for a given transverse spatial resolution is roughly equal to two (polarizations) times the product of the two lattice periods of the PC divided by the spatial resolution squared. With desktop computers, if a few seconds of processing time is allowed, matrices with a dimension of over a thousand may be manipulated. For frequencies not too far above the lowest photonic bandgaps, the optical wavelength in any of the constituent materials of the PC is not much smaller than any of the two lattice periods of the PC. Then a resolution of a small fraction of a wavelength may easily be obtained on a desktop computer. This resolution is necessary to reproduce the divergence of the electric field at sharp edges [9, 10], and reach convergence for the calculation of BW fields. In calculations with such a resolution not too far above the lowest bandgaps, most of the BW components in the expansions (27) are evanescent BWs, *i.e.*, with imaginary $k^{(m)}_{l,q;p}$.

As already pointed out in [7, 5, 6], to get a numerically well behaved recursion relation for propagation of the Bloch wave (BW) amplitudes and derivatives (the u's) through the slices, it is important not to work with the u's directly, but rather with the impedance matrices $\mathbf{Z}^{(m,s)}$, as in (48). It should also be mentioned that an equally well behaved formulation may be obtained in terms of the scattering matrices $\mathbf{\Gamma}^{(m,s)}$.

References

[1] S. Hadzialic, S. Kim, A.S. Sudbø, O. Solgaard, *Two-Dimensional Photonic-Crystals Fabricated in Monolithic Single-Crystal Silicon,* IEEE Photonics Technol. Lett., vol. 22(2), pp.67-69 (2010).

[2] S. Hadzialic, S. Kim, F. Sarioglu, A.S. Sudbø, O. Solgaard, *Displacement Sensing with a Mechanically Tunable Photonic Crystal,* IEEE Photonics Technol. Lett., vol. 22(6), pp.1196-1198 (2010).

[3] J. D. Joannopoulos, S. G. Johnson, J. N. Winn, and R. D. Meade, "Photonic Crystals: Molding the Flow of Light," 2nd Ed. (Princeton University Press, New Jersey, 2008).

[4] A. S. Sudbø , "Film mode matching: A versatile method for mode field calculations in dielectric waveguides," *Pure Appl. Opt. (J. Europ. Opt. Soc. A)*, Vol. 2, pp. 211-233 (1993).

[5] A. S. Sudbø , "Improved formulation of the film mode matching method for mode field calculations in dielectric waveguides," *Pure Appl. Opt. (J. Europ. Opt. Soc. A),* Vol. 3, pp. 381-388 (1994).

[6] R Pregla, A Sudbø, and Ph. Sewell, "Mode solvers and related methods," Ch. 1 in G Guekos, Ed., "*Photonic Devices for Telecommunications,*" (Springer, Berlin 1998).

[7] U. Rogge and R. Pregla, "Method of lines for the analysis of dielectric waveguides," *J. Lightwave Technol.*, Vol. 11, pp. 2015-2020 (1993).

[8] J. Blad and A.S. Sudbø, "Evanescent modes in out-of-plane band structure for two-dimensional photonic crystals," *Optics Express,* vol. 17, pp. 7170–7185 (2009).

[9] J. van Bladel, *Singular electromagnetic fields and sources*, Ch. 4, (Clarendon Press, Oxford, 1991).

[10] A. S. Sudbø , "Why are accurate computations of mode fields in rectangular dielectric waveguides difficult?" *J. Lightwave Technol.*, Vol. 10, pp. 418-419 (1992).

[11] D. Marcuse, *Theory of Dielectric Optical Waveguides*, 2nd Ed. (Academic Press, San Diego, 1991).

[12] W. Schlosser and H. G. Unger, "Partially filled waveguides and surface waveguides of rectangular cross section," *Advances in Microwaves*, pp. 319-387 (Academic, New York, 1966).

[13] T. Itoh (editor), *Numerical techniques for microwave and millimeter-wave passive structures* (Wiley, New York, 1988).

[14] R. Sorrentino, "Transverse resonance technique," Ch. 11 in Itoh's book [13].

[15] R. Pregla and W. Pascher, "The method of lines," Ch. 6 in Itoh's book [13].

[16] M. S. Stern, P. C. Kendall, and P. W. A. McIlroy, "Analysis of the spectral index method for vector modes of rib waveguides," *IEE Proc. J*, Vol. 137, pp. 21-26, 1990.

[17] W. Pascher and R. Pregla, "Analysis of curved optical waveguides by the vectorial method of lines," *17th European Conference on Optical Communication (ECOC '91),* paper TuB5-5, Paris, Sept 9-12, 1991.

[18] A. Dreher and R. Pregla, "Analysis of planar waveguides with the method of lines and absorbing boundary conditions," *IEEE Microw. Guided Wave Lett.*, Vol. 1, pp. 138-140, 1991.

[19] K.A. Zaki, S.W. Chen, and C.Chen, "Modeling discontinuities in dielectric-loaded waveguides," IEEE Trans. Microwave Theory Tech., vol. 36, pp. 1804, 1988.